Supporting Information

Varner et al. 10.1073/pnas.1504102112

SI Text

Modeling Biological Growth. To model the mechanics of mesenchyme-free branching, we constructed a theoretical model for an infinite epithelial layer growing on an underlying gel. As a first approximation, we assumed small deformations and ignored the effects of initial epithelial curvature. Biological growth was included by decomposing the overall deformation in the epithelium into a component due to growth and a component due to elastic deformation. Briefly, within this framework, a 1D tissue element of reference length L_0 is allowed to grow to a new "grown" length L_g, which alters the zero-stress state of the material, and is defined by the growth stretch ratio $\Lambda_g = L_g/L_0$ (Fig. S2). Applied traction forces then deform this grown configuration into the current length L, which invests strain energy in the tissue. This elastic deformation is defined by the elastic stretch ratio $\Lambda^* = L/L_g$. Thus, the overall deformation of the 1D element can be defined using the stretch ratio $\Lambda = L/L_0 = \Lambda^*\Lambda_g$. If small deformations are assumed, mechanical strain can be represented as $\epsilon = \Lambda - 1$, and the overall strain in the tissue ϵ can be approximated by the superposition of the elastic strain ϵ^* and the growth strain ϵ_g, because $\epsilon = \Lambda^*\Lambda_g - 1 = (1+\epsilon^*)(1+\epsilon_g) - 1 \cong \epsilon^* + \epsilon_g$.

Purely Elastic Model. We first considered the case of a growing epithelial layer (with height h, width b, Young's modulus E, Poisson's ratio ν) supported by an elastic foundation (Fig. 3*A*). We incorporated biological growth into the classic equation for the buckling of an infinite elastic layer supported by an elastic half-space (27, 28). Growth of the epithelium was constrained by deformations in the underlying foundation. The mechanical stresses depended only on the elastic strain ϵ^* and were given by $\sigma = E(\epsilon - \epsilon_g)$. Assuming a sinusoidal deflection in the layer, the governing equation takes the form

$$\frac{Eh^3}{12(1-\nu^2)}\frac{d^4v}{dx^4} + N_g h\frac{d^2v}{dx^2} + \gamma\frac{E_f}{2\left(1-\nu_f^2\right)}v = -\frac{d^2M_g}{dx^2},$$

where $v(x)$ is the deflection, γ represents the wave number of the assumed sinusoidal deflection, E_f and ν_f are the elastic modulus and Poisson's ratio of the foundation, respectively, $N_g = bE\int_{-h/2}^{h/2}\epsilon_g(x,y)\,dy$ is the in-plane force due to growth, and $M_g = bE\int_{-h/2}^{h/2} y\epsilon_g(x,y)\,dy$ is the bending moment due to nonuniform growth across the thickness of the layer.

Because no spatial patterns of proliferation were apparent before branching (Fig. 2 *E–G*), we considered the case of uniform growth in the epithelium, $\epsilon_g(x,y) = \epsilon_g^o$, which yielded $M_g = 0$, and $N_g = bEh\epsilon_g^o$. Our governing equation thus simplified to

$$\frac{Eh^3}{12(1-\nu^2)}\frac{d^4v}{dx^4} + N_g h\frac{d^2v}{dx^2} + \gamma\frac{E_f}{2\left(1-\nu_f^2\right)}v = 0.$$

Assuming solutions of the form $v(x) = v_0\cos(\gamma x)$, this gives the characteristic equation

$$N_g = \frac{B}{12}(h\gamma)^2 + \frac{B_f}{2}\frac{1}{(h\gamma)},$$

where $B = E/(1-\nu^2)$ and $B_f = E_f/(1-\nu_f^2)$ represent elastic moduli for the epithelium and surrounding gel, respectively, and depend on the Young's modulus E and Poisson's ratio ν of each material. The system thus reaches instability at a critical in-plane load (due to growth) of

$$N_{g_{cr}} = \frac{3}{4}B_f\sqrt[3]{\frac{B}{3B_f}}$$

and has a dominant wavelength of

$$\lambda_{cr_e} = 2\pi h\sqrt[3]{\frac{B}{3B_f}}.$$

Viscoelastic Model. We extended this model to incorporate the effects of viscoelasticity. In this case, the mechanical properties of the epithelium and foundation were governed by the viscoelastic operators $Q(p)$ and $R(p)$, and $Q_f(p)$ and $R_f(p)$, respectively, where $p = \partial/\partial t$ (45). Using the correspondence principle (46), this yielded the following governing equation:

$$B(p)\frac{h^3}{12}\frac{d^4v}{dx^4} + N_g h\frac{d^2v}{dx^2} + \frac{\gamma B_f(p)}{2}v = 0,$$

where $B(p) = 4Q(p)[Q(p)+R(p)]/(2Q(p)+R(p))$, and $B_f(p)$ is defined similarly (28).

Assuming solutions of the form $v(x) = v_0\cos(\gamma x)$, this produced the characteristic equation

$$N_g = B(p)\frac{(h\gamma)^2}{12} + \frac{1}{2(h\gamma)}B_f(p).$$

The system reached instability at a critical in-plane force (due to growth) of

$$N_{g_{cr}} = \frac{3}{4}B_f(p)\sqrt[3]{\frac{B(p)}{3B_f(p)}}$$

and had a dominant wavelength given by

$$\lambda_{cr} = 2\pi h\sqrt[3]{\frac{B(p)}{3B_f(p)}}.$$

For simplicity, we considered a growing elastic layer supported by a Maxwell-type viscoelastic foundation. The foundation properties were given by $Q_f(p) = G_f p/(p+r_f)$ and $R_f(p) = \infty$, where $r_f = G_f/\mu_f$, G_f is the shear modulus of the foundation, and μ_f is its effective viscosity. In this case,

$$B_f(p) = \frac{4G_f p}{p+r_f}.$$

For the elastic layer, the viscoelastic operators $Q(p)$ and $R(p)$ reduced to the Lamé constants μ_L and λ_L, respectively, which gave

$$B = \frac{4\mu_L(\mu_L+\lambda_L)}{2\mu_L+\lambda_L} = \frac{E}{1-\nu^2}.$$

In this case, the dominant wavelength of the instability was given by

$$\lambda_{cr_v} = 2\pi h\left(\frac{B(p+r_f)}{12G_f p}\right)^{1/3}$$

and critical in-plane load due to growth was $N_{g_{cr}} = 3\left(\frac{G_f p}{p+r_f}\right)\left(\frac{B(p+r_f)}{12G_f p}\right)^{1/3}$. Reorganizing these expressions yields

$$\lambda_{cr_v} = \pi h\left(\frac{2B}{3}\right)^{1/3}\left(\frac{(p+r_f)}{12G_f p}\right)^{1/3}$$

and

$$(N_{g_{cr}})^{-1/2}\left(\frac{2}{3}\right)^{1/3} B^{1/6} = \left(\frac{(p+r_f)}{12G_f p}\right)^{1/3}.$$

Substituting for $\left(\frac{(p+r_f)}{12G_f p}\right)^{1/3}$, we can remove p from our expression for the dominant wavelength and show that

$$\lambda_{cr_v} = \pi h\sqrt{\frac{B}{N_{g_{cr}}}}.$$

This equation indicates that, in the case of a viscoelastic foundation, the dominant wavelength is independent of the material properties of the foundation. Rather, it depends on the in-plane load $N_{g_{cr}}$, which is a linear function of ϵ_g.

Model of Time History of Epithelial Folding. The onset of this growth-induced instability can be initiated by tiny irregularities in the initial deflection of the epithelial layer. If this "noise" is decomposed into Fourier components, those components with wavelengths that correspond to the dominant wavelength of the instability will grow the fastest and become visible. (To the best of our knowledge, this basic idea was first proposed by Biot (47) to explain the onset of folding instabilities during tectonic mechanics.)

Following Biot et al. (48), we simulated this initial noise $v_0(x)$ by creating N peaks at random (and overlapping) locations along the layer, with amplitudes randomly selected between $-\hat{v}_0$ and $\hat{v}_0$. The resulting noise in the deflection was represented using the Fourier integral

$$v_0(x) = \int_0^\infty e^{-\gamma a}\left(\sum_{i=1}^{N}\phi_i\hat{v}_0\cos[\gamma(x-\hat{x}_i)]\right)d\gamma,$$

where N represents the number of peaks, a is a measure of peak width, $\hat{x}_i$ is the randomly generated location for an individual peak (between the values of 0 and L, the length of the layer), $\hat{v}_0$ is the amplitude of the fluctuations, and ϕ_i is a randomly selected variable between -1 and 1.

From these initial conditions, the amplitude of the deflection $v(x,t)$ increased exponentially in time by $v(x,t) = v_0 e^{kt}$ where the exponent k was dependent upon how closely the wavelength of each Fourier component corresponded to the dominant wavelength of the instability. For the case of a growing elastic layer on a Maxwell-type foundation, for slow deformations, we get

$$k = \frac{r_f}{2G_f}\left(N_g h\gamma - \frac{B(h\gamma)^3}{12}\right),$$

where h represents the thickness of the layer, γ is related to the wavelength λ of each Fourier component via $\gamma = 2\pi/\lambda$, and (as above) $N_g = bEh\epsilon_g$.

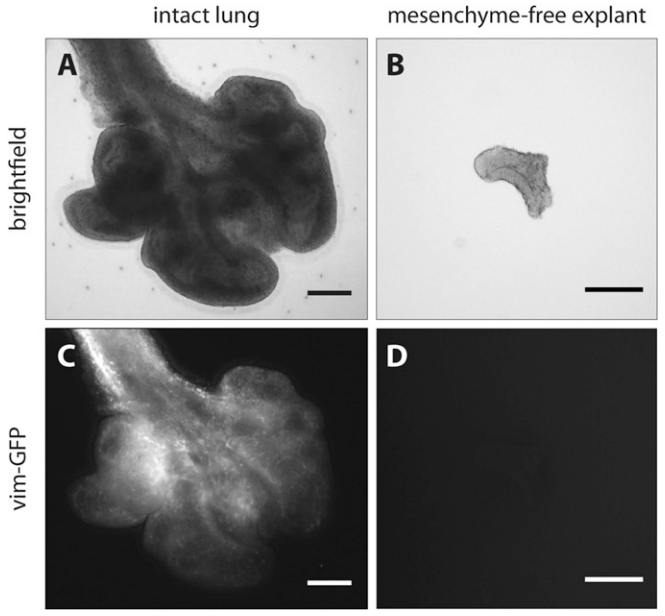

Fig. S1. Epithelial explants isolated from vim-GFP mice at *E*12.5. Bright-field and fluorescent images of explants (*A* and *B*) before and (*C* and *D*) after manual removal of the mesenchyme. Most denuded explants showed no fluorescence, indicating a lack of mesenchymal cells. (Scale bars, 200 μm.)

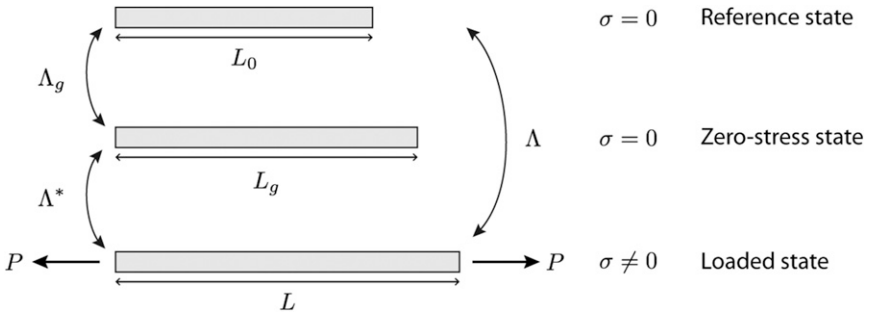

Fig. S2. Schematic depicting linear theory for biological growth. A 1D beam element grows from its reference length L_0 to a new length L_g in a stress-free manner. This changes the zero-stress length from L_0 to L_g and is described by the growth stretch ratio Λ_g. Mechanical loads are then applied to the element at its new, stress-free length L_g. In its final deformed state, the element now has a length L. This second transformation is characterized by the elastic stretch ratio Λ^*. If the overall change in length is given by $\Lambda = L/L_0$, then $\Lambda = \Lambda^* \Lambda_g$. For small deformation, $\Lambda = 1 + \epsilon = (1 + \epsilon^*)(1 + \epsilon_g)$. Neglecting higher-order terms, this yields $\epsilon = \epsilon^* + \epsilon_g$.

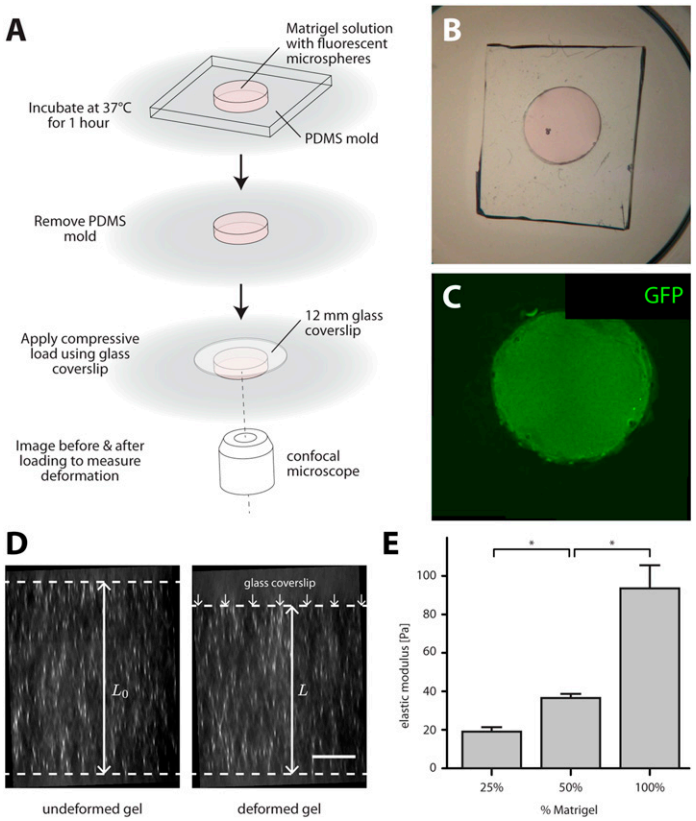

Fig. S3. Measuring the mechanical properties of the gel. (*A*) Schematic of unconfined compression tests. A PDMS mold was used to create specimens of defined cylindrical geometry, which were mechanically loaded with a 12-mm-diameter glass coverslip. Fluorescent microspheres (500 nm in diameter) were suspended within the specimen, before gelation, to observe the gel deformations after loading. (*B* and *C*) Representative image of cylindrical gel specimen (*B*) within the PDMS mold and (*C*) after mold removal. (*D*) Fluorescent image of gel specimen before and after loading. (Scale bar, 200 μm.) (*E*) Measured elastic modulus as a function of Matrigel concentration. Error bars indicate SD. Statistics computed using one-way ANOVA with Tukey's post hoc test; $^*P < 0.05$. These values are similar to those reported elsewhere for Matrigel (49, 50).

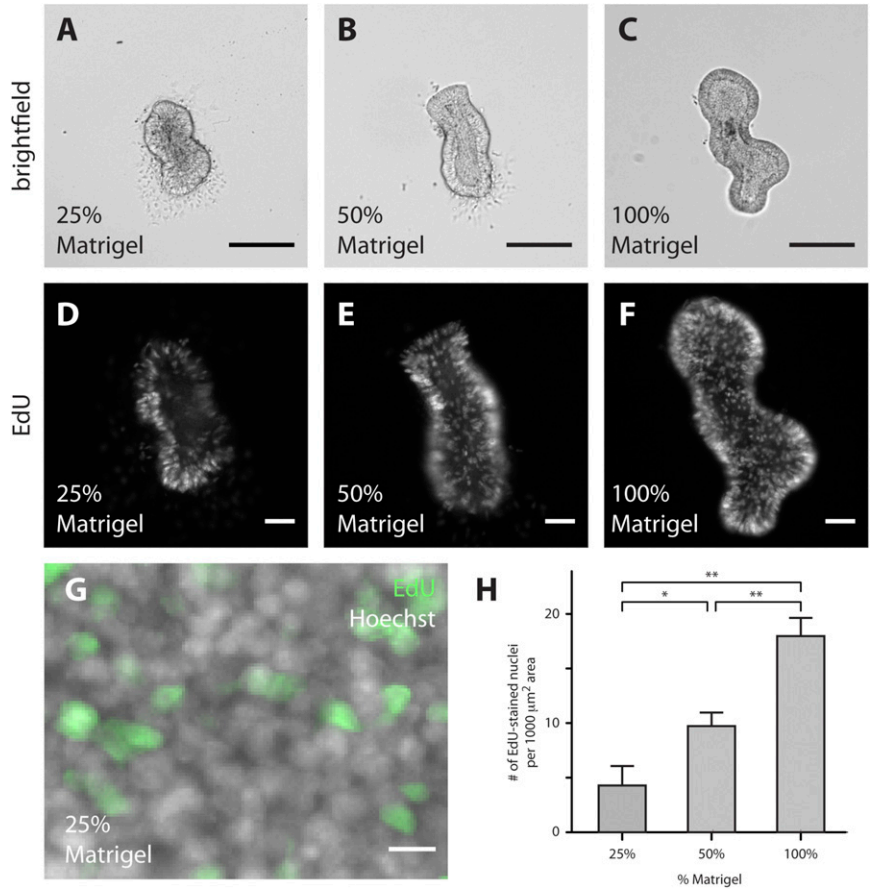

Fig. S4. Quantifying epithelial proliferation rates at different concentrations of Matrigel via EdU incorporation. (*A*–*C*) Epithelial explants after 16 h of culture in gels consisting of (*A*) 25%, (*B*) 50%, and (*C*) 100% Matrigel. (Scale bars, 200 μm.) (*D*–*F*) Fluorescent images of EdU incorporation in explants cultured in gels consisting of (*D*) 25%, (*E*) 50%, and (*F*) 100% Matrigel. (Scale bars, 50 μm.) (*G*) Composite high-magnification images of EdU and Hoechst labeling. (Scale bar, 10 μm.) (*H*) Epithelial proliferation rate as a function of Matrigel concentration. The number of EdU-stained nuclei was normalized with respect to the cumulative area of the regions of interest analyzed within each explant. Error bars indicate SD. Statistics computed using one-way ANOVA with Tukey's post hoc test; $*P < 0.05$; $**P < 0.01$.

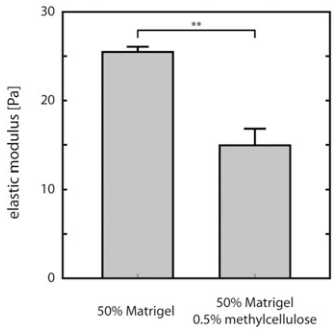

Fig. S5. Altering the mechanical properties of the gel using methylcellulose. Measured elastic modulus of gels containing either 50% Matrigel or 0.5% methylcellulose and 50% Matrigel. Shown are mean ± SD for four experimental replicates. Statistics computed using Student's *t* test; $**P < 0.01$.

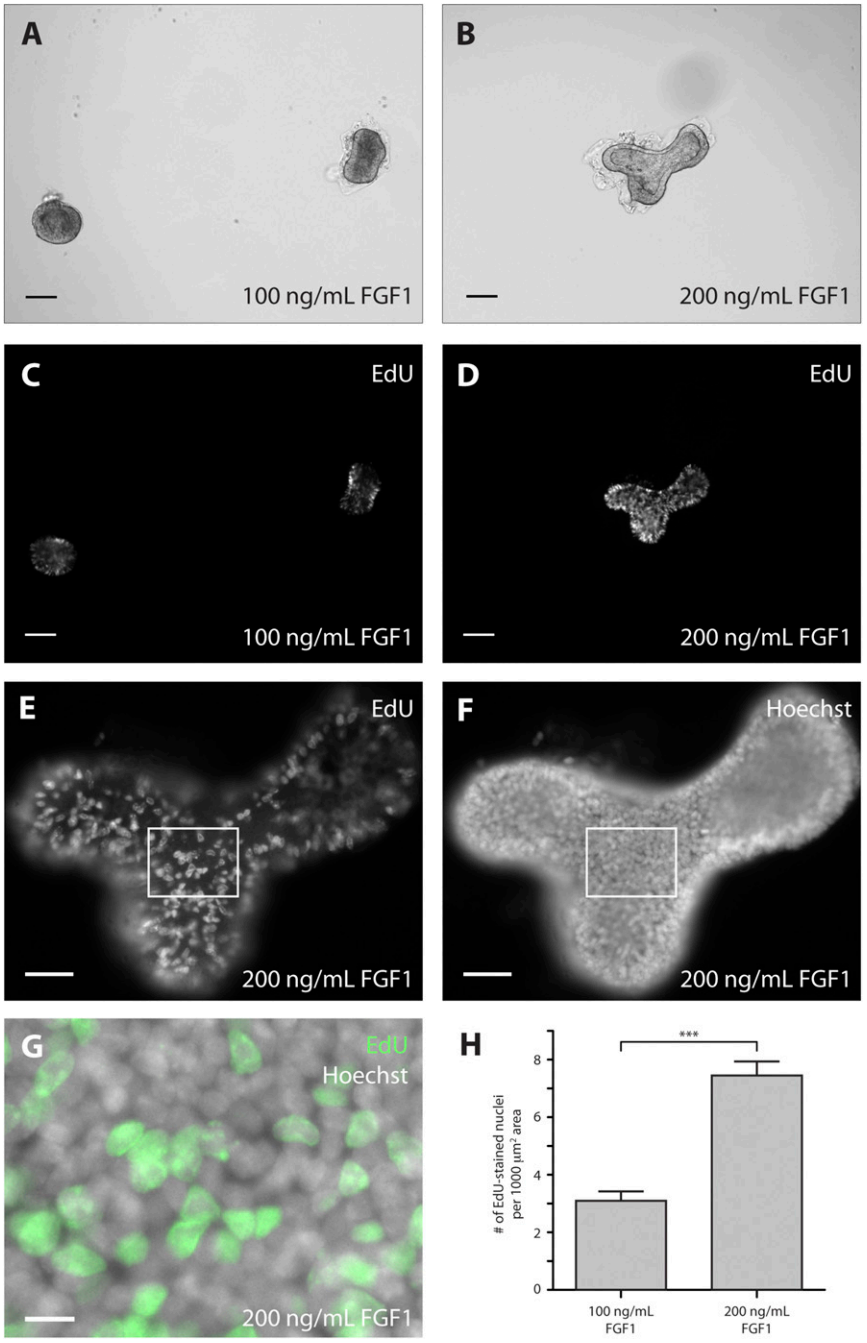

Fig. S6. Quantifying epithelial proliferation rates at different concentrations of FGF in 100% Matrigel. (*A*–*D*) Epithelial explants after 16 h of culture in the presence of (*A* and *C*) 100 ng/mL and (*B* and *D*) 200 ng/mL FGF1. Explants were pulsed with EdU for 1 h before fixation. (*A* and *B*) Bright-field and (*C* and *D*) fluorescent images showing EdU incorporation at low magnification. (Scale bars, 250 μm.) (*E* and *F*) Explants were costained for (*E*) EdU and (*F*) Hoechst 33258 to quantify proliferation rates. (Scale bar, 50 μm.) (*G*) Composite high-magnification image of white boxed region shown in *E* and *F*. Hoechst 33258-labeled nuclei (grayscale) are shown overlayed with those positive for EdU incorporation (green). (Scale bar, 10 μm.) (*H*) Epithelial proliferation rates as a function of FGF concentration. The number of EdU-stained nuclei was normalized with respect to the cumulative area of the regions of interest analyzed within each explant. Error bars indicate SD. Statistics computed using Student's *t* test; ***$P < 0.001$.

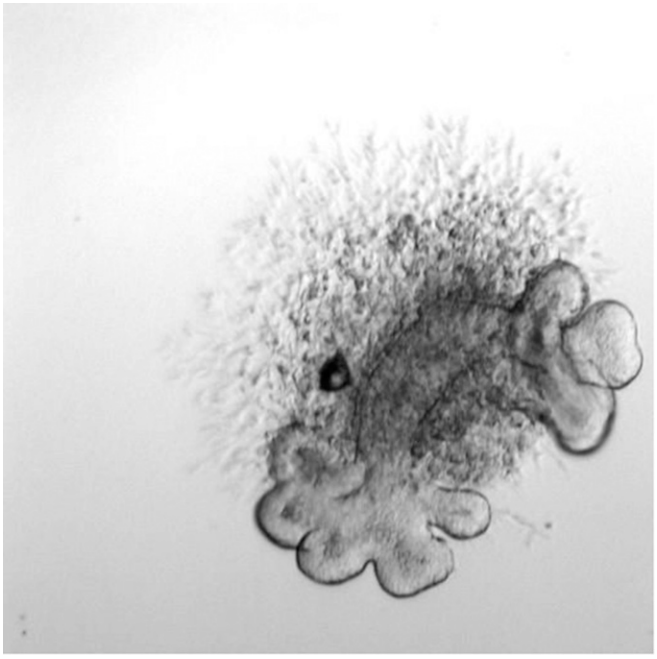

Movie S1. Morphodynamics of mesenchyme-free branching during ~48 h of culture.

Movie S1

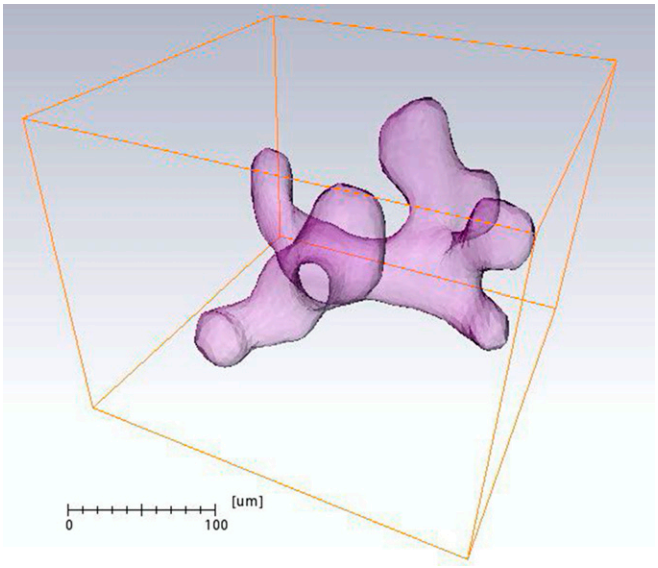

Movie S2. Creating epithelial surface reconstructions using confocal imaging data.

Movie S2